Investigation of Critical Stress Intensity Factors for AISI 4340 and ASTM A533 Alloy Steels at Different Murakami Area Parameters

Azzam D. Hassan [1], Yahya Muhammed Ameen [2], M. A. Mohammed [1], and Raheem Al-Sabur [2,*]

[1] Materials Department, Engineering College, University of Basrah, Basrah 61004, Iraq
[2] Mechanical Department, Engineering College, University of Basrah, Basrah 61004, Iraq
Email: azzam.hassan@uobasrah.edu.iq (A.D.H.); yahya.ameen@uobasrah.edu.iq (Y. M.A); mohammed.abedlhafd@uobasrah.edu.iq (M.A.M); raheem.musawel@uobasrah.edu.iq (R.A.-S.)
*Corresponding author

***Abstract*—This study's main goal is to find out how minor defects affect the development of fatigue cracks in metallic materials by examining the Murakami area parameter's ($\sqrt{area}$) effect on the spread of fatigue cracks in ASTM A533-B1 and AISI 4340 steel alloys. The threshold stress intensity factor (ΔK_{th}) is analyzed at two loading ratios (R = 0.1 and R = 0.5). The findings indicated that the ΔK_{th} increases for a range of $\sqrt{area}$ values and then tends to be constant. At low ΔK values, the ΔK_{th} change is effective on the fatigue crack growth range and disappears gradually as ΔK increases at ΔK_{th} = 7.80 MPa$\sqrt{m}$ (no defect) or ΔK_{th} = 4.78 MPa$\sqrt{m}$ (small defect). For the AISI 4340 steel, the crack growth rate response (in case of no defects) compared with the crack growth rate response (with minimal defect). Unlike the case of AISI 4340 alloy steel, there is no correlation between the values and an increase in the value of ΔK for ASTM A533-B1 alloy steel. According to their critical values, the ASTM A533-B1 alloy steel has a lower value than the AISI 4340 alloy steel, where the critical values are the value of (ΔK) at which the crack growth response curves with and without impurities start to match. These values remained constant for each material regardless of changes in (ΔK_{th}) but decreased as the R ratio increased.**

***Keywords*—stress intensity factor, murakami area parameter, crack growth rate, fatigue, AISI 4340, ASTM A533**

I. Introduction

Knowledge of fatigue behavior authorizes engineers to design components that can withstand cyclic loads without sudden failure, improving durability and dependability. It's crucial to understand that fatigue cracks can have severe consequences if they occur in large-scale structures like bridges. These cracks can lead to sudden, catastrophic failures in critical structures like vehicles and aircraft [1]. The presence of multiple cracks introduces complex interactions that can significantly affect load distribution and stress concentration, necessitating advanced analytical techniques. Understanding these factors is vital for enhancing safety, extending service life, and optimizing maintenance strategies in these industries. Fatigue Crack Growth (FCG) prediction is critical for assessing fracture mechanics and structural integrity. The process indicates the crack steps: initiation, propagation, and final fracture. Several factors influence FCG behavior, including load ratio, environment, temperature, and microstructure [2, 3]. In the fatigue crack growth prediction studies, the Fatigue Crack Growth (FCG) rate (da/dN) is a key parameter used in determining the remaining lifetime or a suitable inspection interval for a component [4].

In contrast, the crack growth starts under cyclic loading conditions ΔKth parameter plays a crucial role in fatigue analysis [5]. Understanding the threshold stress intensity factor (ΔK_{th}) is critical for predicting the onset of crack growth, which is essential for ensuring the reliability and longevity of elements constructed from this material. Minor defects or flaws in steel can significantly affect the crack propagation rate due to the stress concentration they create. These imperfections can act as initiation points for cracks, especially under cyclic loading conditions [6]. Determining small natural defects, such as those generated by porosity in casting or pits created by metal corrosion conditions, is extremely difficult. Therefore, Murakami's work to find a specific methodology for the effect of such defects on fatigue strength is of enormous importance. Murakami related the size of small defects to the concept of $\sqrt{area}$, where the square root of the expected area of small defects is the direction of fatigue strength, as shown in Fig. 1. The Murakami area parameter $\sqrt{area}$ is an essential factor in the study of steel alloys because it gives a clear view and a deeper understanding of mall defects or non-metallic inclusions that influence fatigue strength and fracture toughness under critical stress intensity factors. Thus, it makes it possible to predict stress concentration and fatigue crack propagation in specific areas or in the general structure of steel alloys that are widely used, especially in aerospace, automotive, and structural applications.

Manuscript received August 21, 2024; revised September 26, 2024; accepted December 10, 2024; published March 20, 2025.

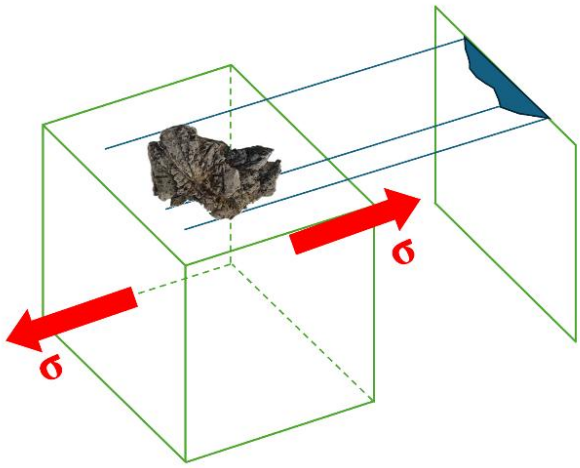

Fig. 1. Murakami model for small defects as $\sqrt{area}$.

Most steel alloys, including high- or low-carbon steel or even alloy steel, suffer from corrosion problems in different environments, which exposes their use in engineering applications such as fatigue applications to corrosion cracks [7, 8]. AISI 4340 steel is a high-strength, low-alloy steel typically used in aerospace, automotive, and structural applications due to its outstanding mechanical properties [9]. The AISI 4340, martensitic steel, is susceptible to the effects of stress corrosion cracking [10]. Due to the importance of fatigue crack growth rate in AISI 4340 steels, studies on it began seriously in the late last century [11, 12].

Despite abundant research on the critical stress intensity factor of steel alloys, it is still an intriguing topic from several other directions, such as notch fatigue and size effect using stress field intensity [13]. Residual stresses significantly influence steel alloys' fatigue crack growth rate, particularly when exposed to various environments, including harsh marine conditions. Manufacturing processes such as welding, machining, or surface treatments often introduce these stresses, which can either act as beneficial compressive stresses or detrimental tensile stresses around the crack tip. Aggressive factors such as saltwater, high humidity, and fluctuating temperatures exacerbate residual stress effects in marine environments [14]. Moreover, earnest attempts are to model the threshold stress intensity factor to predict fatigue endurance reliability [15]. In various transportation industries, the stress intensity factor analysis remains critical for assessing the behavior of multiple cracks in orthotropic steel structures. These materials, renowned for their directional mechanical properties, find widespread application in components such as bridges, rail tracks, and vehicle frames, where precise crack propagation prediction is crucial for maintaining structural integrity [16]. The study of small defects, especially the so-called blunt notch, and its effects on fatigue life evaluation is significant in bridge design and predicting defect formation [17].

Experimental studies have shown that the initial defects—such as their depth, width, and shape—are crucial in determining the fatigue crack propagation rate. For instance, a defect with a more significant depth, smaller width, and sharper morphology accelerates the crack propagation rate. The majority of studies have focused on the variation in stress intensity factors. Kujawski and Ellyin [18] developed a model for predicting fatigue crack propagation that considers the material's bulk cyclic and low-cycle fatigue properties. This model specifically addresses the effects of the R-ratio on fatigue crack growth at intermediate and low-stress intensities. Their model is based on the idea that the product of plastic strain and stress measures the plastic strain energy density in the "process zone", which determines fatigue failure. Their analysis delves into the stress ratio at the crack-tip region, proposing relationships that describe its variation along the crack line. They were close when the model's predictions were compared to experimental data. This showed that the model captured the basic mechanics of fatigue crack growth well when stress ratios changed. Rihan *et al.* [19] used a new fracture mechanics method to find the threshold stress intensity factor (KIscc) for heat-treated AISI 4340 steels in 3.5% NaCl solutions at room temperature. They did this by using small circumferential notch tensile specimens. Their KIscc determination was confirmed to be 15 MPa√m, which is very close to values obtained by others using standard specimens. Weng *et al.* [20] tried more environments by checking the effect of Corrosion Fatigue Crack Growth (CFCG) of AISI 4340 in dry air and in distilled water, besides the 3.5% NaCl aqueous solution used by Rihan *et al.* [19]. Furthermore, they investigated the effect of variation of R-ratios (the ratio of minimum to maximum load in a cycle) and loading frequencies. They concluded that the environmental impact was practical whenever the maximum stress intensity factor (K_{max}) exceeded the threshold stress intensity for stress corrosion cracking (KIscc). Ryder and Gallagher [21] looked at the static and cyclic crack growth behavior of AISI 4340 steel in distilled water at several different temperatures. They discovered the CFCG rate was about ten times higher than the dry air cyclic crack growth rate at 25 °C. Also, when ΔK (the stress intensity factor range) stayed the same, the CFCG rates for the different stress intensity factors were less than or the same as the static growth rates. The modified El-Haddad model was the focus of an extensive experimental study by Patriarca *et al.* [22] to explore the effect of fatigue crack growth on the fatigue model incorporating results in the threshold region at different load ratios starting from low values (R = −2.5) up to relatively high values (R = 0.7). They validated it against constant amplitude fatigue experiments for AISI 4340 steel. Li *et al.* [23] proposed theoretical modifications to a Fatigue Crack Growth (FCG) model concentrating on local damage accumulation. Their study presents a new relationship for FCG, which predicts stage II FCG behavior independently of the basic low-cycle fatigue properties. This new relationship suggests a more accurate prediction of crack growth rates. Kalnaus *et al.* [24] used different concentrations of NaCl aqueous solutions to study the effects of corrosion environment on stress corrosion cracking in AISI 4340 steel. They found that the NaCl

concentration in distilled water has significant implications for understanding and preventing stress corrosion cracking in this type of steel where the threshold stress intensity factors appeared independent of the NaCl concentration. Xu *et al.* [25] divided the fatigue crack propagation study under high-cycle torsional loads into two stages: the early crack propagation stage, where quantitative analyses of fracture processes were used, and the later crack propagation stage, where deflection analyses were used. They found that when the mode I stress intensity factor exceeded the threshold value, the initiated crack would branch into a multi-mode I crack. Calvín *et al.* [26] looked at how the stress intensity factor and crack closure affect the effective stress intensity factor range. They achieved this by comparing analytical and numerical calculation methods incorporating experimentally determined crack shapes. They also found that crack closure more strongly influences the effective stress intensity factor range distribution than the maximum stress intensity factor. Hickey *et al.* [27] quantified the effects of testing frequency on Fatigue Crack Growth Rates (FCGRs) in AISI 4340. They found that crack growth rates accelerated with decreasing frequency in fully aerated fresh water and identified stress corrosion cracking as the dominant mechanism at lower frequencies. Li *et al.* [28] indicated using SEM and X-ray that the crack growth behavior in AISI 4340 steels under monotonic loading shows that crack growth distance and critical load rise with fracture toughness, and the crack growth direction angles vary with tempering temperatures up to 500 °C. Xu *et al.* [29] investigated the nucleation of microstructural fatigue cracks in AISI 4340 steel, focusing on the early stages of crack initiation. They found that the initiated crack plane generally aligned with the maximum shear stress plane.

Storm and Abou-Hanna [30] explored methods to simplify determining stress intensity factors while maintaining high accuracy based on the Murakami equation. Their study investigated multiple-notch geometries with varying crack lengths to assess their effectiveness. The method got errors from −10.03% to 8.94% compared to exact analytical solutions. Based on the Murakami model, Ben *et al.* [31] studied the relationship between the printing defect and fatigue crack growth in the SLM-Ti6Al4V alloy and concluded that the fatigue life was not significantly affected by cyclic annealing of the specimens within a good range of stress intensity factor (ΔK), which contributed to a deeper understanding of the competitive failure mechanisms generated between internal and surface defects. According to Landron *et al.* [32], the local stress level and the Murakami parameter are crucial in explaining gradient effects in critical crack cases in $AlSi_9Cu_3$ alloy components, particularly in high cycle fatigue and under fully reversed tension-compression conditions. Oberreiter *et al.* [33] used root squared area (Murakami's model) to predict the fatigue resistance and maximum stress intensity factor ΔK_{max} in the aluminum alloy during wire arc additive manufacturing. They found that fatigue resistance was highly affected by larger-size flaws.

Although studies on stress intensity factors in fatigue conditions in ferrous metals are extensive, the effect of varying Murakami area parameter ($\sqrt{area}$) values on critical stress intensity factors in steel alloys remains limited and needs more in-depth research. The current study predicts the behavior of two widely used steel alloys (AISI 4340 and ASTM A533) in the presence of minor defects, represented by the Murakami area parameter model. Moreover, the present study modified the FCG model proposed by Kujawski and Ellyin. In this modification, a new relation has been derived to examine the change in the fatigue crack growth rate with the shift of minor defects, especially when the change in loading ratios was considered with its effect on the ΔK_{th} and the fatigue crack growth.

The present study will review the mechanical properties and chemical compositions of the alloys used, followed by a review of the equations used. The effects of changing the Murakami area parameter ($\sqrt{area}$) on the threshold stress intensity factor will be discussed in the discussion part. Then, a comprehensive comparison of the values of fatigue crack growth depending on the effect of loading ratios and small defects will be made.

II. Materials and Theoretical Background

This study investigated the threshold stress intensity factor (ΔK_{th}) at different loading ratios (R = 0.1 and R = 0.5) using AISI 4340 high-strength, low-alloy steel. Tables I and II display the chemical composition and mechanical properties of AISI 4340, respectively.

TABLE I. Chemical Composition of AISI 4340 Wt % [24]

Ni	Cr	C	Mo	Mn	Fe
1.82	0.70	0.37	0.21	0.71	Balance

TABLE II. Mechanical Properties of AISI 4340 Steel at R = 0.1 and R = 0.5

Properties	Value
Cyclic strain hardening exponent (n')	0.146
Elastic modulus (E) (MPa)	209
Yield stress ($\acute{\sigma}_y$) (MPa)	724
Fatigue strength coefficient ($\acute{\sigma}_f$) MPa	1713
Fatigue ductility exponent (c)	−0.650
Fatigue ductility coefficient ($\acute{\epsilon}_f$)	0.830
Fatigue strength exponent (β)	0.745

The threshold intensity factor represents the minimum stress intensity required for a crack to propagate. Below this threshold, the crack remains dormant or grows exceptionally slowly. It serves as a critical parameter in predicting the fatigue life of materials, especially in the presence of cracks. Researchers study fatigue crack growth behavior under various loading conditions (e.g., constant amplitude, variable amplitude) to determine the threshold. Experimental tests involve applying cyclic loads to specimens with pre-existing cracks. The crack growth rate is monitored as a function of the stress intensity factor (K) or its components (K_I, K_II, K_III) near the crack tip. The transition from subcritical (below threshold) to critical (above threshold) crack growth is analyzed. Factors

affecting the threshold include material properties, loading frequency, environment, and crack size. The threshold stress intensity factor range defines the minimum value of the stress intensity factor necessary for crack propagation [34]. Kujawski and Ellyin indicated that the da/dN could be calculated from [18]:

$$\frac{da}{dN} = 2\delta^* \left[\frac{\Delta K^2 - \Delta K_{th}^2}{4(1+\acute{n})(\acute{\sigma_f} - \sigma_m^*)\acute{\epsilon_f}\pi E \delta^*}\right]^{\frac{1}{\beta}} \quad (1)$$

where E is elastic modulus, n' is cyclic strain hardening exponent, $\acute{\epsilon_f}$ is fatigue ductility coefficient, $\acute{\sigma_f}$ is fatigue strength coefficient, σ_m^* is local mean stress within fatigue "process-zone" size or material length parameter (δ^*), which is typically taken as constant according to the type of the material [18].

Later, Li *et al.* [23] modified the Kujawski and Ellyin by adding the effect of $\acute{\sigma_y}$ and adjusting the δ^* to be not constant to find a more accurate relation for da/dN-ΔK:

$$\frac{da}{dN} = 2\left(\frac{\Delta K^2 - \Delta K_{th}^2}{\pi E \acute{\sigma_y}}\right)\left[\frac{\acute{\sigma_y}}{4\acute{\epsilon_f}(1+\acute{n})(\acute{\sigma_f} - \sigma_m^*)}\right]^{\frac{1}{\beta}} \quad (2)$$

Both models kept the ΔK_{th} as constant, depending on the material type. By comparing the two equations, the relation between $\acute{\sigma_y}$, ΔK, δ^* and can be written as:

$$\acute{\sigma_y} = \frac{\Delta K^2 - \Delta K_{th}^2}{\pi E \delta^*} \quad (3)$$

The Murakami area parameter model $\sqrt{area}$ is a well-known tool in the scientific community for predicting the fatigue strength of metallic materials with minute flaws [35]. The threshold stress intensity factor range (ΔK_{th}) for cracks or defects (measured in MPa·√m) is considered a variable and can be computed using the method proposed in [36, 37] .

$$\Delta K_{th} = 3.3 \times 10^{-3}(HV + 120)\left(\sqrt{area}\right)^{\frac{1}{3}}\left(\frac{1-R}{2}\right)^{\alpha} \quad (4)$$

HV is Vickers hardness, and R is loading ratio influence, which refers to the ratio of the minimum applied load to the maximum applied load during a fatigue cycle [38]. In that regard, A critical threshold for the stress intensity factor range ΔK_{th}(critical) could be established to account for the minimum size of defects that may cause significant damage [39].

III. Result and Discussion

According to Eq. (4), for R = 0.1 and HV =389 kg_f/mm^2 (for AISI 4340 steel), the ΔK_{th} can be measured as a function of $\sqrt{area}$. Table III shows the threshold stress intensity factor change according to the area parameter model variation. According to Eq. (4), as the area parameter increases, the ΔK_{th} increases for a range of values of the area parameter model and then tends to be constant [35], which are 7.80 MPa√m, for R = 0.1 and 3.60 MPa√m, for R = 0.5. Table III gives the impression that for both cases of loading ratio (R = 0.1) and (R = 0.5) when the hardness is constant, the threshold stress intensity factor (ΔK_{th}) decreases with decreasing Murakami area parameter model $\sqrt{area}$. Studies often use the $\sqrt{area}$ to estimate fatigue strength in small defects and surface cracks, which is calculated as the square root of the projected area of the defect crack. The ΔK_{th} decreases as $\sqrt{area}$ decreases can be understood by considering the principles of crack growth and fatigue behavior in materials. The ΔK_{th} represents the material's resistance to fatigue crack propagation under cyclic loading, and more minor defects of $\sqrt{area}$ mean there is less initial damage present in the material. Moreover, smaller defects typically result in a higher threshold stress intensity factor, which allows the materials to endure higher cyclic stress levels before the growth of the fatigue crack. The smaller defects in an area can lead to extended fatigue life, delayed crack initiation, control of the crack propagation rate, and enhanced defect tolerance.

TABLE III. Threshold Stress Intensity Factor according to Eq. (4) at R = 0.1 and 0.5

At loading ratio (R = 0.1)		At loading ratio (R = 0.5)	
$\sqrt{area}$	ΔK_{th}	$\sqrt{area}$	ΔK_{th}
200	7.14	52	3.60
150	6.48	50	3.55
100	5.66	45	3.43
90	5.47	40	3.30
80	5.26	35	3.16
70	5.03	25	2.82
60	4.78	20	2.62

For both cases (R = 0.1 and R = 0.5), the values of E, $\acute{\sigma_y}$, $\acute{\epsilon_f}$, n, $\acute{\sigma_f}$, and β kept constant (see Table II), while ΔK_{th} for R = 0.1 and R = 0.5 are calculated from Eq. (4) (see Table III). Tables IV and V indicate the fatigue crack growth da/dN results as compared with the corresponding values obtained from Eqs. (1) or (2) for R = 0.1 and R = 0.5, respectively.

TABLE IV. Fatigue Crack Growth Comparison between Current Model and [18, 23] Models for R = 0.1 (ΔK_{TH} in (MPa√m)

x-ΔK	Without defects at Kth = 7.80	With small defect at Kth = 4.78
	da/dN (m/cycle)109	da/dN (m/cycle)109
200	7.14	52
8.7900	0.0255	0.0846
9.2810	0.1541	0.3858
9.5310	0.5373	1.2181
9.7840	2.6338	5.5039
11.3650	7.8892	12.2789
13.5930	12.8947	16.8506
14.7890	23.1769	28.7587
18.5420	40.8533	46.3424
20.7600	57.4077	63.3043
30.5500	159.2640	166.2040
36.5380	260.3130	268.0800
49.3970	564.8640	573.8900
63.7070	1,094.3600	1,104.7700

TABLE V. FATIGUE CRACK GROWTH COMPARISON BETWEEN CURRENT MODEL AND [18, 23] MODELS FOR R = 0.5 (ΔKTH IN (MPA√M)

x-ΔK	Without defects at Kth = 7.80	With small defect at Kth = 4.78
	da/dN (m/cycle)109	da/dN (m/cycle)109
3.9860	0.0253	0.0512
4.2530	0.1990	0.3154
4.3320	0.4750	0.7208
4.6720	0.8070	1.0806
4.8040	1.5900	2.0687
5.6420	2.7100	3.1410
6.5010	4.9600	5.4740
8.9680	10.0000	10.4456
11.0440	14.1000	14.4464
14.6660	33.6000	34.0752
20.0370	89.8000	90.5257
29.8140	207.0000	207.2800
33.7130	296.0000	296.7520
3.9860	0.0253	0.0512

The fatigue crack growth rate (da/dN) describes how quickly a crack advances per loading cycle. Therefore, the description (da/dN) of AISI 4340 steels is fundamental. The results obtained from Tables IV and V highlight that the fatigue crack growth rate (da/dN) increases with increasing stress intensity factor (ΔK), regardless of the low or high loading cycle R-ratios (R = 0.1 and R = 0.5) for two cases, K_{th} = 7.80 MPa√m (no defect) and ΔK_{th} = 4.78 MPa√m (small defect). In case of small defects, tiny cracks, inclusions, or micro-voids may be present, which are stress concentration foci and hence, the ability of the material to withstand applied cyclic stress will be low. On the contrary, the absence of all types of defects in the material will be an important factor in reducing the presence of concentrated stresses and, hence, a higher ability to withstand applied cyclic stress and a longer life until crack formation and growth.

At low ΔK values, the change in ΔK_{th} is effective where there is a difference in the values of (da/dN), while this difference begins to disappear gradually as ΔK increases either at K_{th} = 7.80 MPa√m (no defect) and K_{th} = 4.78 MPa√m (small defect). It is also noted that the increase (da/dN) is gradual at low values of ΔK up to 13.5930 MPa√m, but there is a sharp increase in the values and a faster growth of (da/dN). It can be interpreted as the stress intensity factor depending on the load applied, the specimen's geometry, and the crack's size, and the crack growth rate increases rapidly, leading to unstable crack growth and eventual fracture of the material. In steel alloys, this behavior of a gradual and then sharp increase in the rate of fatigue crack growth (da/dN) with increasing stress intensity range (ΔK) is influenced by the microstructural properties of the material. Steel alloys often contain various microstructural barriers, such as grain boundaries, dislocations, and precipitates, influencing how cracks initiate and propagate. The microstructural properties of the material can explain this behavior in steel alloys, as these alloys often include precipitates of alloying materials, dislocations, and grain boundaries, which generate various microstructural barriers that influence the rate of fatigue crack growth. When ΔK is low, these barriers absorb energy and slow the propagation. In contrast, when ΔK is excessively high, microstructural barriers become less effective at impeding crack growth.

Looking at the overall behavior, it becomes clear that it is similar to the behavior at a low ratio (R = 0.1). Moreover, it is noted that the fatigue crack growth rate (da/dN) is meager compared with corresponding values at R = 0.1, even though there is no defect (ΔK_{th} = 3.60 MPa√m) or a small defect (ΔK_{th} = 3.15 MPa√m).

A. *Effect of Loading Ratios*

The high load ratio (R) and the stress intensity factor are closely related, as R represents the ratio between the lowest and highest stress intensity factor values. Consequently, it significantly influences the stress intensity factor, which impacts the fatigue crack growth rate. This section is based on the absence of the small defect, as its effect will be studied more extensively in the following section. Fig. 2(a) reveals that a high R ratio (R = 0.5) yields faster fatigue crack growth rate than a low R ratio (R = 0.1). However, this rate gradually decreases until a significant convergence occurs whenever the stress intensity factor range (ΔK) values increase.

The overall behavior of the obtained results for AISI 4340 steels is consistent with the experimental results obtained by Kujawski and Ellyin [18] and Glinka [40], as indicated in Fig. 2(b), representing reliable validation.

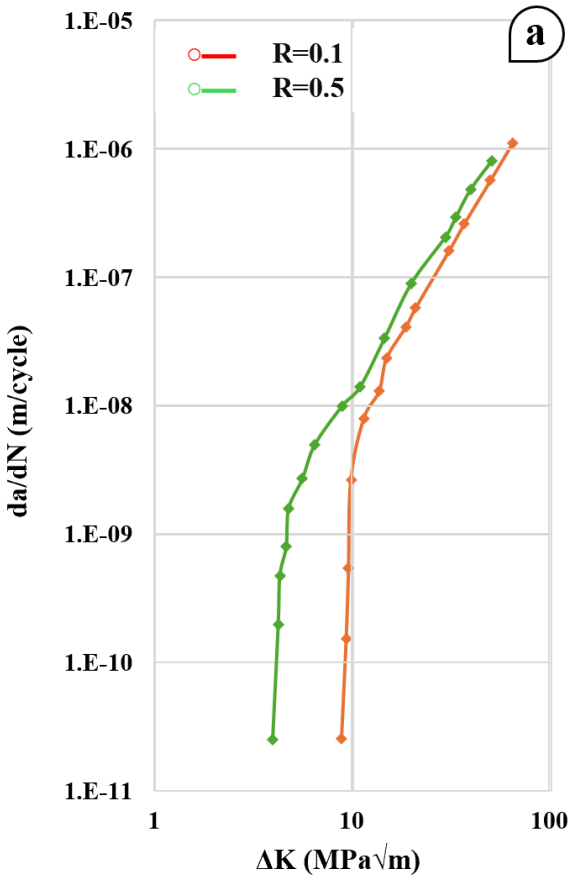

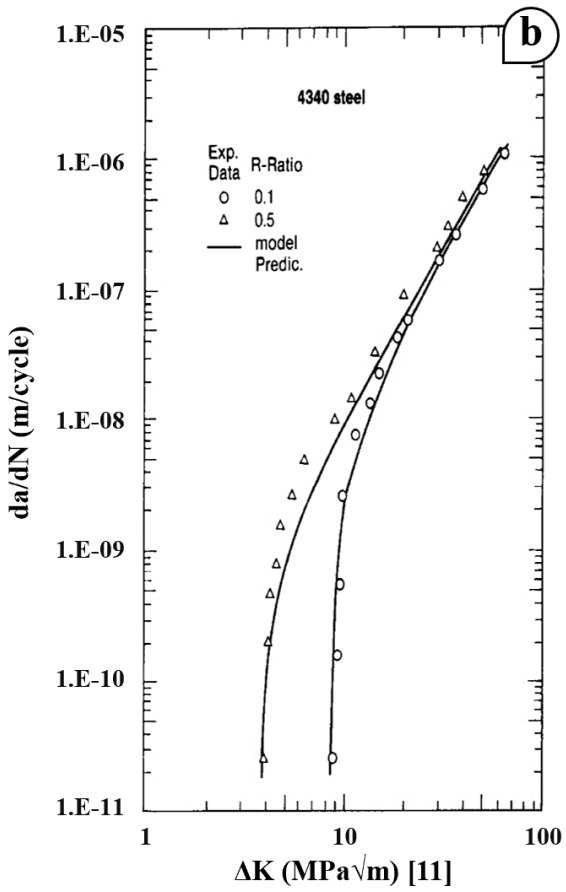

Fig. 2. Effect of R ratios on the fatigue crack growth rate of 4330 steel at R = 0.1 and R = 0.5 (a) current study, (b) results from Ref. [18].

B. *Effect of Small Defects*

The $\sqrt{area}$ is often relied upon to study the effect of small defects on fatigue crack growth rate. It is particularly relevant in assessing fatigue life and crack growth from small defects. Therefore, using the $\sqrt{area}$ will allow for adjusting the stress intensity factor (ΔK) to account for the influence of small cracks or defects. This section will rely on the results previously mentioned in Table III. Small defects will be compared with the absence of defects for all cases of the R ratio. For R = 0.1, the ΔK_{th} = 7.80 MPa√m represents a no-defect case, while for R = 0.5, the ΔK_{th} = 3.60 MPa√m represents a no-defect case. For R = 0.1, four threshold stress intensity factor (ΔK_{th}) cases were inspected, 7.14, 6.48, 5.66, and 5.47 MPa√m, which correspond to $\sqrt{area}$ values of 200, 150, 100, and 90, respectively, as shown in Fig. 3(a)–(d). All cases were not merged into one figure due to close values and the difficulty of comparison, so each case was taken separately and compared with the case of no defects, which represents ΔK_{th} = 7.80 MPa√m for cases where R = 0.1.

It is observed that there is similar behavior in all cases. It is summarized by the apparent effect of small defects when the stress intensity factor (ΔK) values are low (x-axis) in Fig. 3(a)–(d). However, this effect becomes similar to the impact of the absence of defects when the stress intensity factor values are high. Obtaining the values at which the behavior change occurs represents the critical stress intensity factor. This value is essential because it gives an impression of the crack growth speed and its effect on the metal. When all cases are followed in this figure, the value of ΔK of 30.5500 MPa√m emerges as a distinctive value, as no matter how the threshold stress intensity factor (ΔK_{th}) values differ or the $\sqrt{area}$ values change, the crack growth rate will be matched approximately, see also Table IV. Therefore, ΔK of 30.5500 MPa√m represents the critical value of AISI 4340 steel at R = 0.1, as shown in Table VI.

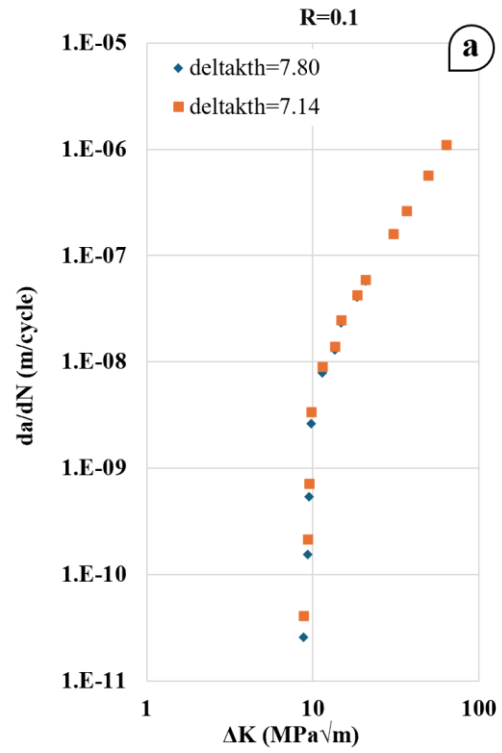

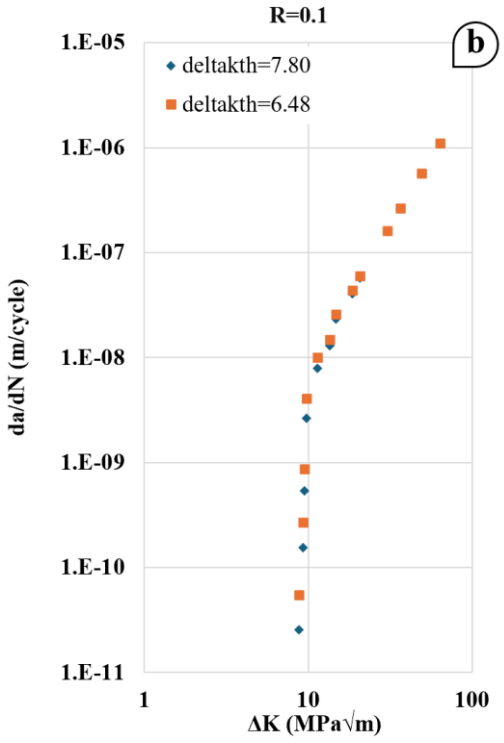

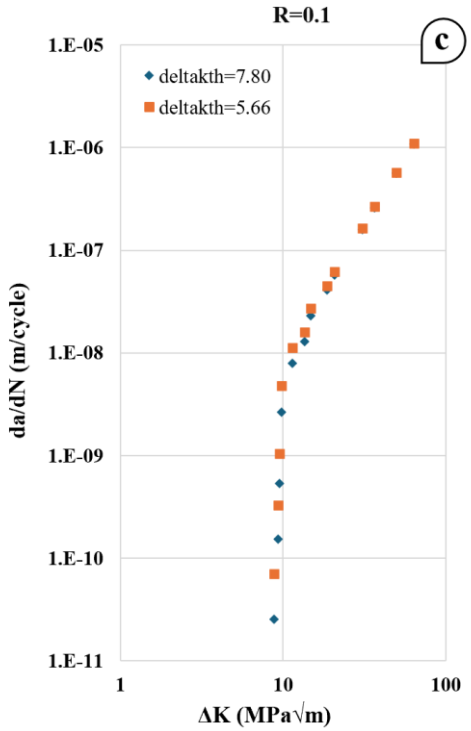

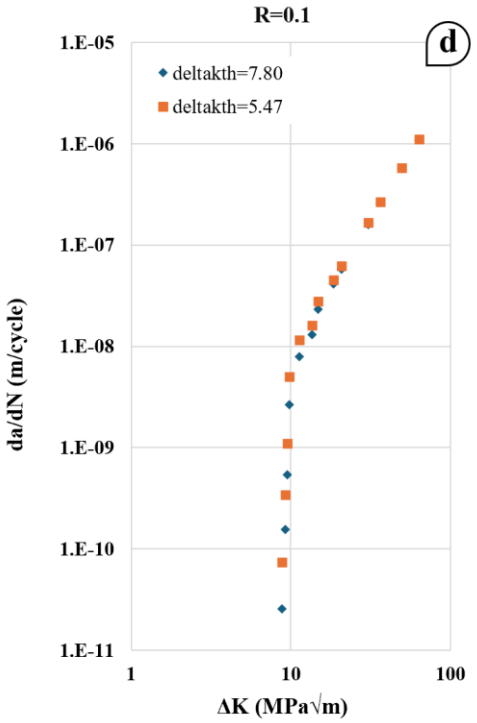

Fig. 3. Effect of threshold stress intensity factor variation of the crack propagation at R=0.1 for AISI 4340 steels at (a) ΔK_{th}=7.14, (b) ΔK_{th}=6.14, (c) ΔK_{th}=5.66, and (d) ΔK_{th}=5.47.

Fig. 3(a)–(d) show that the behavior response with the presence of the defects will shift in the y-axis and will be above the behavior response without defects. Moreover, there is a value of ΔK (in the x-axis), and the responses below this value showed mismatching while the responses above it showed matching. Table VI shows that the critical value of ΔK is constant with different values of ΔK_{th}.

When the loading ratio increased to R = 0.5, ΔK_{th} = 3.60 MPa√m represented a no-defect case. Four threshold stress intensity factor (ΔK_{th}) cases were inspected: 3.55, 3.43, 3.30, and 3.16 MPa√m, corresponding to $\sqrt{area}$ values of 50, 45, 40, and 35, respectively, as shown in Fig. 4(a)–(d).

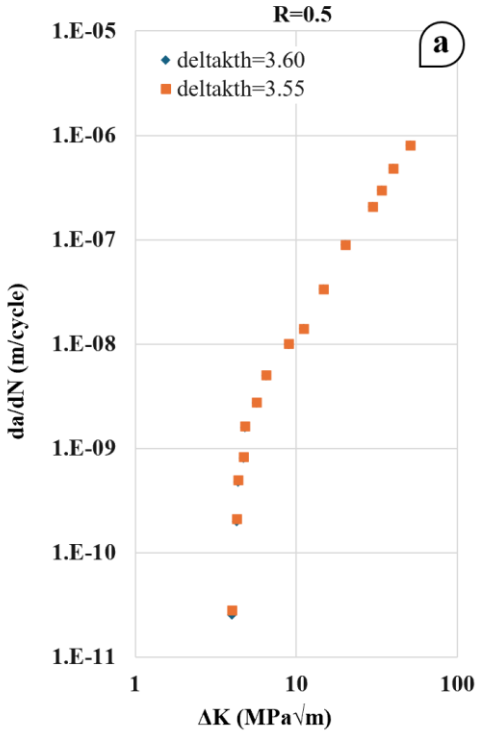

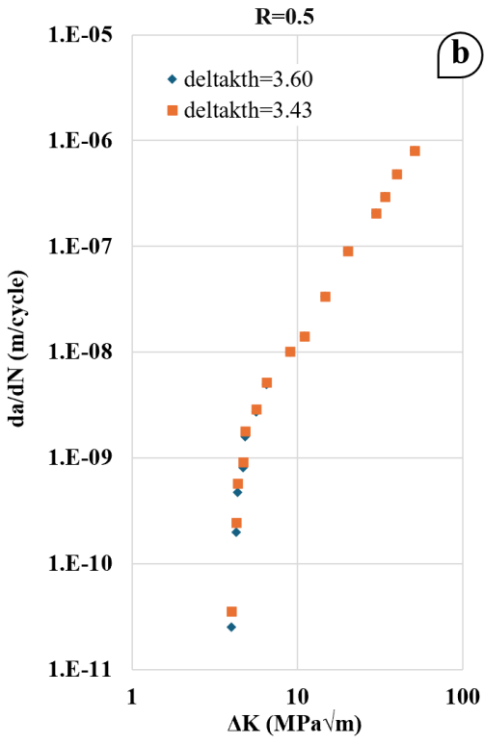

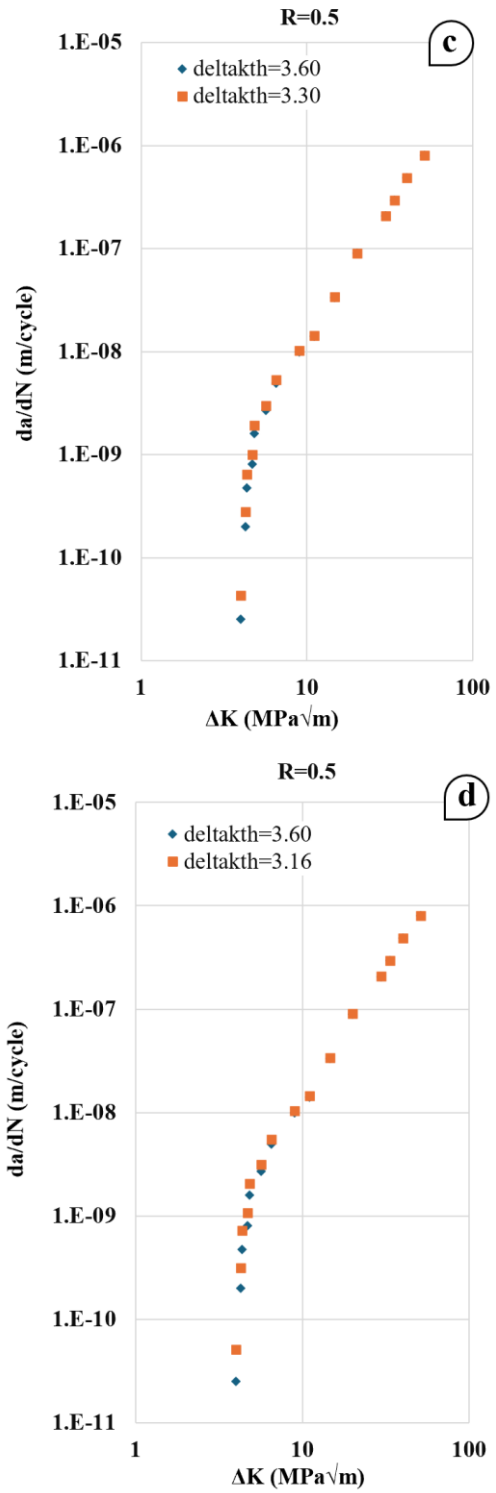

Fig. 4. Effect of threshold stress intensity factor variation of the crack propagation at R = 0.5 for AISI 4340 steels (a) ΔK_{th}=3.55, (b) ΔK_{th}=3.34, (c) ΔK_{th}=3.33, and (d) ΔK_{th}=3.16.

The general behavior of the fatigue crack growth rate (da/dN) relationship was not affected by the stress intensity factor (ΔK), despite the increase in the value of loading ratio to 0.5 and the significant decrease that occurred in the value of (ΔK_{th}) and √area. An apparent lack of convergence between the state of the presence of defects and the state of their absence continues to occur when ΔK is low, and then convergence begins to increase as this value increases. However, the vital observation in this context is that the critical ΔK value decreased by more than 50% to ΔK of 29.8100 MPa√m. Also, in this case, this value did not change regardless of the changes in the values of (ΔK_{th}) and √area, which indicates that it is the critical value for AISI 4340 steels at R = 0.5, as shown in Table VI.

TABLE VI. CRITICAL VALUES OF ΔK FOR AISI 4340 STEELS (UNITS IN MPA√M)

At loading ratio (R = 0.1)		At loading ratio (R = 0.5)	
ΔKth	**critical ΔK**	**ΔKth**	**critical ΔK**
7.14	30.5500	3.55	29.8100
6.48	36.5380	3.43	29.8100
5.66	36.5380	3.30	29.8100
5.47	36.5380	3.16	29.8100

C. Critical Stress Intensity Factors of ASTM A533-B1 Alloy Steel

To enhance the scope and applicability of the study, it was extended to include another type of steel alloy, where the critical ΔK of ASTM A533-B1 alloy was explored. This alloy was selected based on its qualitative differences from AISI 4340 alloy steel in terms of manganese and nickel values. Specifically, ASTM A533-B1 has a high manganese content (1.15–1.50%) and a low nickel content (0.37–0.87%), whereas AISI 4340 Alloy Steel has a lower manganese content (0.60–0.80%) and a higher nickel content (1.65–2.00%). This difference gave the two alloys different properties, especially in tensile strength, leading to various applications.

The choice of ASTM A533-B1 and AISI 4340 steel alloys in this study since both alloys have an equal ΔK_{th} when impurities are absent in the AISI 4340 alloys, which allows for a good validation of the equations obtained in this research and the possibility of comparing the behavior of the two materials in the presence of impurities.

The results previously obtained for AISI 4340 alloy steel indicated that the loading ratio (R) did not significantly affect the general behavior of the fatigue crack growth rate (da/dN) but only affected the reduction of critical ΔK values. Therefore, when studying the ASTM A533-B1 alloy steel, the test will only be conducted on the value one for the loading ratio (R = 0.1). The ΔK_{th} = 7.70 MPa√m represents a no-defect case corresponding to an √area of 170. Three threshold stress intensity factor (ΔK_{th}) cases were inspected: 7.55, 5.66, and 5.47 MPa√m, corresponding to $\sqrt{area}$ values of 160, 150, and 130, respectively, as shown in Table VII.

The most important result from the effects of small defects on crack growth propagation for ASTM A533-B1 alloy steel (as shown in Fig. 5(a)–(d) is that there is no correlation between the values and an increase in the value of K, unlike the case of AISI 4340 alloy steel. In addition, the increase in crack growth propagation continued gradually as the value of ΔK increased for all ΔK_{th} cases, which is also a different behavior than what happened with AISI 4340 alloy steel, where there was a sharp increase in crack growth propagation when ΔK increased.

TABLE VII. CRITICAL STRESS INTENSITY FACTORS OF ASTM A533-B1 ALLOY STEEL

$\sqrt{area}$	ΔK_{th}	Critical ΔK
170	7.70	No defect
160	7.55	17.62
150	7.39	17.62
130	7.04	17.62
170	7.70	No defect

The mechanical properties, particularly tensile strength and elongation, can explain this. The ASTM A533-B1 alloy steel has better properties than the AISI 4340-alloy steel, making it more resistant to crack growth. Moreover, ASTM A533-B1 alloy steel behaved similarly to AISI 4340 alloy steel in the presence of a critical value for the stress intensity factor so that it is not affected by the change in ΔK_{th}. In addition, it can be observed that ΔK reached 17.62 MPa√m in this case, which is about 48% less than AISI 4340 alloy steel for the case of R = 0.1.

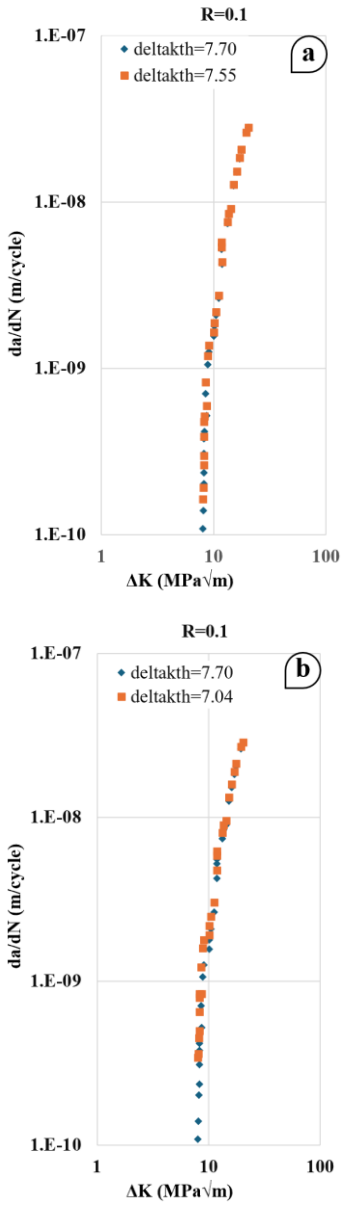

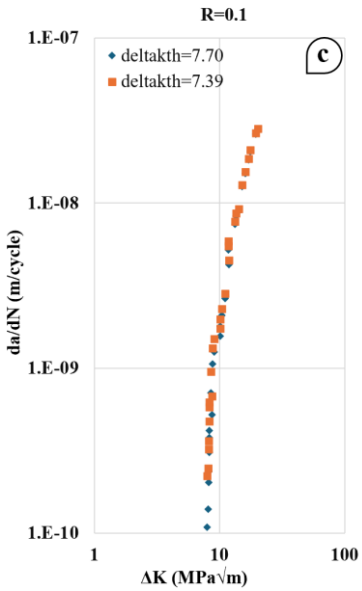

Fig. 5. Effect of threshold stress intensity factor variation of the crack growth propagation at R = 0.1 for ASTM A533-B1 alloy steel at (a) ΔK_{th}=7.55, (b) ΔK_{th}=7.04, and (c) ΔK_{th}=7.39

IV. CONCLUSION

This study used the variable Murakami area parameter model to look into how small flaws and the threshold stress intensity factor (ΔKth) affect the rate of fatigue crack growth (da/dN). The two types of steel alloys examined in the study were ASTM A533-B1 and AISI 4340. Below is a summary of the main discoveries from the research:

1. Notably, the research considers the Murakami area parameter as a variable rather than a constant, addressing a critical gap in existing studies and providing a more realistic representation of material behavior under varying conditions. Moreover, this study proposed a novel correlation to predict the behavior of AISI 4340 and ASTM A533-B1 steel alloys, enhancing the Kujawski and Ellyin Fatigue Crack Growth (FCG) model by incorporating the influence of the Murakami area parameter, expressed as $\sqrt{area}$.
2. The ΔK_{th} increases for a range of $\sqrt{area}$ values and then tends to be constant. In other words, it was noticed that any changes in the $\sqrt{area}$ values would cause the ΔK_{th} values to become constant depending on the loading cycle. The values reached 7.8 MPa√m for R = 0.1 and 3.6 MPa√m for R = 0.5 and are still the same for all area values.
3. At low ΔK values, the ΔKth change is effective and disappears gradually as ΔK increases either at Kth = 7.80 MPa√m (no defect) and ΔK_{th}= 4.78 MPa√m (small defect). Tiny inclusions, cracks, or micro voids that are stress concentration foci may be present in minor flaws; as a result, the material's capacity to tolerate applied cyclic stress will be reduced.
4. A high R ratio (R = 0.5) yields a faster fatigue crack growth rate than a low R ratio (R = 0.1) and tends to converge with ΔK increase.

5. For AISI 4340 steels at R = 0.1 with different $\sqrt{area}$ values, or ΔK_{th}, a distinctive value of ΔK can be found where the crack growth rate response (No defects) will be matched approximately with the crack growth rate response (with defect). The critical value decreases with the increase in the value of R.
6. The ASTM A533-B1 alloy steel (which has same ΔK_{th} when impurities are absent in the AISI 4340 alloys) has a lower value of critical ΔK than the AISI 4340 alloy steel. These values were found to be constant for each material and were not affected by changes in (ΔK_{th}) while their value de-creased when the R ratio increased.
7. Regarding the significance of the findings, this research contributes substantially to understanding fatigue crack growth behavior in high-strength steels by emphasizing the role of small defects and loading ratios. The improved Kujawski and Ellyin FCG model, which incorporates the Murakami area parameter, serves as a potent predictive tool for assessing fatigue behavior across a wide spectrum of loading cycles and defect dimensions. In other words, the developed model in this study, which is based on the Kujawski and Ellyin FCG model, gave good results compared to the previous models; in addition, this model can be used for both types of steel alloys AISI 4340 and ASTM A533-B1 to determine the threshold stress intensity factor variation of the crack growth propagation and for a wide range of loading cycles as well as a divergent value of the Murakami area parameter model $\sqrt{area}$ which was not addressed in previous studies.

V. Study Contributions and Implications

This section discusses this study's main contributions, limitations, and future recommendations. The main contributions are:

1. Adding the variable Murakami area parameter to the FCG model completes our understanding of how small flaws affect the progression of fatigue cracks, giving us new ideas that previous research didn't.
2. The results show the importance of considering small flaws and changing load ratios when evaluating fatigue. This can yield accurate predictions and better material performance in essential engineering applications.
3. Using variable Murakami area parameter led to more accurate results than depending on constant values in previous studies.

It is worth noting that this study was limited to two types of steel alloys (AISI 4340 and ASTM A533-B1 steels), which is considered a major determinant. The study also relied on the results of previous experimental tests. Therefore, applying the resulting relationships to other steel or iron alloys requires deeper research and more experiments.

For future studies, examining a more comprehensive range of Murakami area parameter values could yield greater insight into the model's limitations and applicability. Moreover, upcoming research should explore the relevance of the developed model to further steel alloys and ferrous metals. More studies are required to verify the model's relevance to other materials that possess varying microstructural features. Enlarging the research to include various alloys and defect dimensions could strengthen the model's reliability. Exploring the influence of environmental aspects such as temperature and corrosion on the growth of fatigue cracks might also yield significant insights.

Finaly, it is important to note here that this study is related to two steel alloys with similar properties, especially when impurities are absent in the AISI 4340 alloys. Confirming that the developed model can be used for other steel alloys or ferrous metals requires a deeper study. Using the relationships developed in this study, exploring other alloys could be a future goal. Also, using a wider range of Murakami area parameter values could give a better understanding of the developed model's usability and limitations.

Conflict of Interest

The authors declare no conflict of interest.

Author Contributions

Conceptualization, A.D.H. and Y. M.A ; methodology, A.D.H. ;software R.A.-S.; validation, R.A.-S., and A.D.H. ; formal analysis, R.A.-S., M.A.M; investigation, A.D.H., and M.A.M ; resources, A.D.H. and Y. M.A; data curation, R.A.-S., M.A.M; writing—original draft preparation, R.A.-S., M.A.M; writing—review and editing, A.D.H. and Y. M.A ; visualization, R.A.-S. ; supervision, R.A.-S. All authors have read and agreed to the published version of the manuscript.

References

[1] N. M. Chowdhury, J. Wang, W. K. Chiu, and P. Chang, "Static and fatigue testing bolted, bonded and hybrid step lap joints of thick carbon fibre/epoxy laminates used on aircraft structures," *Compos. Struct.*, vol. 142, 2016. https://doi.org/10.1016/j.compstruct.2016.01.078

[2] D. F. Laurito, C. A. R. P. Baptista, M. A. S. Torres, and A. J. Abdalla, "Microstructural effects on fatigue crack growth behavior of a microalloyed steel," *Procedia Engineering*, 2010. https://doi.org/10.1016/j.proeng.2010.03.206

[3] D. Huang *et al*., "Modeling of temperature influence on the fatigue crack growth behavior of superalloys," *Int. J. Fatigue*, vol. 110, 2018. https://doi.org/10.1016/j.ijfatigue.2017.12.020

[4] J. Lansinger, T. Hansson, and O. Clevfors, "Fatigue crack growth under combined thermal cycling and me-chanical loading," *Int. J. Fatigue*, vol. 29, no. 7, 2007. https://doi.org/10.1016/j.ijfatigue.2006.10.024

[5] S. Kolitsch, H. P. Gänser, and R. Pippan, "Determination of crack initiation and crack growth stress-life curves by fracture mechanics experiments and statistical analysis," *Procedia Structural Integrity*, 2016. https://doi.org/10.1016/j.prostr.2016.06.379

[6] Y. Murakami and M. Endo, "Effects of defects, inclusions and inhomogeneities on fatigue strength," *Int. J. Fatigue*, vol. 16, no. 3, 1994. https://doi.org/10.1016/0142-1123(94)90001-9

[7] H. M. Lieth, R. Al-Sabur, R. J. Jassim, and A. Alsahlani, "Enhancement of corrosion resistance and mechan-ical properties of API 5L X60 steel by heat treatments in different environments," *Journal of Engineering Re-search (Kuwait)*, vol. 9, no. 4B, 2021, https://doi.org/10.36909/jer.14591

[8] H. M. Lieth, M. A. Jabbar, R. J. Jassim, and R. Al-Sabur, "Optimize the corrosion behavior of AISI 204Cu stainless steel in different environments under previous cold working and welding," *Metallurgical Research and Technology*, vol. 120, no. 4, 2023. https://doi.org/10.1051/metal/2023058

[9] J. G. Lima, R. F. Ávila, A. M. Abrão, M. Faustino, and J. P. Davim, "Hard turning: AISI 4340 high strength low alloy steel and AISI D2 cold work tool steel," *J. Mater Process Technol*., vol. 169, no. 3, 2005. https://doi.org/10.1016/j.jmatprotec.2005.04.082

[10] N. Eliaz, A. Shachar, B. Tal, and D. Eliezer, "Characteristics of hydrogen embrittlement, stress corrosion cracking and tempered martensite embrittlement in high-strength steels," *Eng. Fail Anal.*, vol. 9, no. 2, 2002. https://doi.org/10.1016/S1350-6307(01)00009-7

[11] S. K. Putatunda and J. M. Rigsbee, "Effect of specimen size on fatigue crack growth rate in AISI 4340 steel," *Eng. Fract Mech*, vol. 22, no. 2, 1985. https://doi.org/10.1016/S0013-7944(85)80034-5

[12] A. S. Khan and T. K. Paul, "A new model for fatigue crack propagation in 4340 steel," *Int. J. Plast*, vol. 10, no. 8, 1994. https://doi.org/10.1016/0749-6419(94)90022-1

[13] Y. L. Wu, S. P. Zhu, J. C. He, D. Liao, and Q. Wang, "Assessment of notch fatigue and size effect using stress field intensity approach," *Int. J. Fatigue*, vol. 149, 2021. https://doi.org/10.1016/j.ijfatigue.2021.106279

[14] H. Xin and M. Veljkovic, "Residual stress effects on fatigue crack growth rate of mild steel S355 exposed to air and seawater environments," *Mater Des*., vol. 193, 2020. doi: 10.1016/j.matdes.2020.108732

[15] X. Guan, "Probabilistic modeling of threshold stress intensity factor for fatigue endurance reliability prediction," *Probabilistic Engineering Mechanics*, vol. 72, 2023. https://doi.org/10.1016/j.probengmech.2023.103417

[16] H. Zhang, H. Liu, and H. Kuai, "Stress intensity factor analysis for multiple cracks in orthotropic steel decks rib-to-floorbeam weld details under vehicles loading," *Eng. Fail Anal.*, vol. 164, 108705, Oct. 2024. https://doi.org/10.1016/j.engfailanal.2024.108705

[17] R. Hao, P. Lehto, and W. Lin, "Critical distance-based fatigue life evaluation of blunt notch details in steel bridges," *J. Constr Steel Res*., vol. 201, 2023. https://doi.org/10.1016/j.jcsr.2022.107738

[18] D. Kujawski and F. Ellyin, "A fatigue crack growth model with load ratio effects," *Eng. Fract. Mech*, vol. 28, no. 4, 1987. https://doi.org/10.1016/0013-7944(87)90182-2

[19] R. Rihan, R. K. Singh Raman, R. N. Ibrahim, and D. Gerrard, "Determination of the threshold stress intensity factor (K Iscc) of 4340 steel using small circumferential notched tensile (CNT) specimens," in *Proc. 46th Annual Conference of the Australasian Corrosion Association*, 2006: Corrosion and Prevention 2006, 2006.

[20] L. Weng, J. Zhang, S. Kalnaus, M. Feng, and Y. Jiang, "Corrosion fatigue crack growth of AISI 4340 steel," *Int. J. Fatigue*, vol. 48, 2013. https://doi.org/10.1016/j.ijfatigue.2012.10.015

[21] J. T. Ryder and J. P. Gallagher, "Environmentally controlled fatigue crack-growth rates in sae 4340 steel—Temperature effects," *Journal of Basic Engineering*, 1970.

[22] L. Patriarca, M. Filippini, and S. Beretta, "Short-crack thresholds and propagation in an AISI 4340 steel under the effect of SP residual stresses," *Fatigue Fract Eng. Mater Struct.*, vol. 41, no. 6, 2018. https://doi.org/10.1111/ffe.12771

[23] D. M. Li, W. J. Nam, and C. S. Lee, "An improvement on prediction of fatigue crack growth from low cycle fatigue properties," *Eng. Fract Mech*, vol. 60, no. 4, 1998. https://doi.org/10.1016/S0013-7944(98)00029-0

[24] S. Kalnaus, J. Zhang, and Y. Jiang, "Stress-corrosion cracking of AISI 4340 steel in aqueous environments," *Metallurgical and Materials Transactions A: Physical Metallurgy and Materials Science*, 2011. https://doi.org/10.1007/s11661-010-0335-y

[25] Z. K. Xu, B. Wang, P. Zhang, X. Z. Gu, and Z. F. Zhang, "Crack branching and deflection in AISI 4340 steel under cyclic torsional loading," *Materials Science and Engineering: A*, vol. 863, 2023. https://doi.org/10.1016/j.msea.2022.144561

[26] G. Calvín, M. Escalero, H. Zabala, and M. Muñiz-Calvente, "A new effective stress intensity factor approach to determine thickness-independent fatigue crack growth rate curves," *Theoretical and Applied Fracture Mechanics*, vol. 121, 2022. https://doi.org/10.1016/j.tafmec.2022.103505

[27] W. F. Hickey, M. Rahimi, B. Cowan, and T. Nguyen, "On the effects of test frequency and crack driving force on the crack growth rate behavior of 4340 steel," in *Proc. AMPP Corrosion, AMPP*, 2023,

[28] H. F. Li, X. P. Wang, Y. M. Liu, Y. Q. Liu, P. F. Liu, and S. P. Yang, "Crack growth path of high-strength steel with different toughness under monotonic and cyclic loadings," *Int. J. Fatigue*, vol. 169, 2023. https://doi.org/10.1016/j.ijfatigue.2023.107503

[29] Z. Xu, B. Wang, P. Zhang, Y. Zhu, X. Wang, and Z. Zhang, "Crack initiation mechanism of AISI 4340 steel for high-cycle torsional fatigue loading," *Steel Res. Int.*, vol. 94, no. 8, 2023. https://doi.org/10.1002/srin.202200976

[30] B. Storm and J. J. Abou-Hanna, "Linearized layering method for stress intensity factor determination," *SN Appl. Sci.*, vol. 5, no. 5, 2023. https://doi.org/10.1007/s42452-022-05225-3

[31] D. D. Ben, H. J. Yang, H. B. Ji, D. L. Lian, L. X. Meng, J. Chen, J. L. Yi, L. Wang, J. T. M. De Hosson, R. Yang, and Z. F. Zhang, "Fatigue crack growth behavior in additive manufactured Ti6Al4V alloy with intentionally embedded spherical defect," *Materials Science and Engineering: A*, vol. 885, 145612, 2023. https://doi.org/10.1016/j.msea.2023.145612

[32] T. Landron, F. Morel, N. Saintier, V. D. Le, D. Bellett, P. Osmond, and A. Forré, "The combined effects of a heterogeneous porosity distribution and stress gradient on the high cycle fatigue behavior of high pressure die cast AlSi9Cu3," *International Journal of Fatigue*, vol. 182, 108212, 2024. https://doi.org/10.1016/j.ijfatigue.2024.108212

[33] M. Oberreiter, N. N. Abidin, N. N. Khaleeda, M. Stoschka, Y. H. P. Manurung, M. S. Adenan, and R. R. Krishnamoorthy, "Analytical prediction of fatigue resistance of additively manufactured aluminium alloy based on Murakami method," *Journal of Applied Engineering Design & Simulation (JAEDS)*, vol. 3, no. 2, pp. 1–14, 2023. https://doi.org/10.24191/jaeds.v3i2.66

[34] L. Duarte, M. Madia, and U. Zerbst, "The effect of the environmental conditions on the threshold against fatigue crack propagation," *Procedia Structural Integrity*, 2021. https://doi.org/10.1016/j.prostr.2022.03.030

[35] M. Endo, "Effects of hardness and crack geometry on δkthof small cracks," *Journal of the Society of Materials Science*, vol. 35, no. 395, 1986. https://doi.org/10.2472/jsms.35.911

[36] Y. Murakami, *Metal Fatigue: Effects of Small Defects and Nonmetallic Inclusions*, Academic Press, 2019. https://doi.org/10.1016/C2016-0-05272-5

[37] B. M. Schönbauer and H. Mayer, "Effect of small defects on the fatigue strength of martensitic stainless steels," *Int. J. Fatigue*, vol. 127, 2019, https://doi.org/10.1016/j.ijfatigue.2019.06.021

[38] B. L. Boyce and R. O. Ritchie, "Effect of load ratio and maximum stress intensity on the fatigue threshold in Ti-6Al-4V," *Eng. Fract. Mech.*, vol. 68, no. 2, 2001. https://doi.org/10.1016/S0013-7944(00)00099-0

[39] B. M. Schönbauer, K. Yanase, and M. Endo, "The influence of various types of small defects on the fatigue limit of precipitation-hardened 17-4PH stainless steel," *Theoretical and Applied Fracture Mechanics*, vol. 87, 2017. https://doi.org/10.1016/j.tafmec.2016.10.003

[40] G. Glinka, "A notch stress-strain analysis approach to fatigue crack growth," *Eng. Frac.t Mech.*, vol. 21, no. 2, 1985. https://doi.org/10.1016/0013-7944(85)90014-1